Sensing and Bio-Sensing Research 47 (2025) 100725

Contents lists available at ScienceDirect

Sensing and Bio-Sensing Research

journal homepage: www.elsevier.com/locate/sbsr

Cost-effective Amperometric Immunosensor for cardiac troponin I as a step towards affordable point-of-care diagnosis of acute myocardial infarction

Niamh Docherty [a,*], Lilian Collins [a], Susan Pang [b], Ying Fu [c], Stuart Milne [d], Damion Corrigan [a]

[a] University of Strathclyde, Centre for Advanced Measurement Science and Health Translation, Pure and Applied Chemistry, Thomas Graham Building, 295 Cathedral St, Glasgow G1 1XL, UK
[b] National Measurement Laboratory at LGC, Queens Road, Teddington, Middlesex TW11 0LY, UK
[c] University of Strathclyde, Pure and Applied Chemistry, Technology Innovation Centre, 99 George Street, Glasgow G1 1RD, UK
[d] University of Strathclyde, Biomedical Engineering, Wolfson Centre, 106 Richmond St, Glasgow G1 1XQ, UK

ARTICLE INFO

Keywords:
Electrochemical Immunosensor
Electrochemical ELISA
Cardiac troponin I
Chronoamperometry
Point of care

ABSTRACT

Early detection of cardiac troponin I in blood is vital for acute myocardial infarction diagnosis. A low-cost thin film gold electrode array was used with affordable ELISA antibodies and reagents to fabricate two cardiac troponin I amperometric immunosensors. The HRP-labelled sandwich immunocomplex was constructed on the gold electrode surface, and chronoamperometry was used to quantify cTnI indirectly by measuring the amount of TMB^{+} produced at the electrode surface. First, the system was evaluated using a physisorption approach to immobilise the capture antibody to the electrode with a 309 pg/mL LOD observed. Subsequently, a second sensor variant was produced using sulfo-LC-SPDP as a crosslinker to control antibody immobilisation, which resulted in an improved sensitivity with an LOD of 109 pg/mL. The chemisorption sensor outperformed the working range of the commercially available ELISA kit used (8000–125 pg/mL), demonstrating the power of enhanced antibody immobilisation and electrochemical detection for clinically relevant levels of cardiac troponin I. Amperometric immunosensors offer vital advantages including being cost-effective, simple to use, and compatible with commercially available reagents. These features make the sensor accessible to users and easy to manufacture. With further improvements to sensitivity and performance in complex samples, the sensor could be deployed to streamline acute myocardial infarction diagnosis and reduce the burden of chest pain patients on the healthcare system.

1. Introduction

Cardiovascular diseases represent 32 % of all global deaths, with an estimated 17.9 million deaths from cardiovascular diseases in 2019 according to the World Health Organisation [1]. Experts project that the burden of heart and circulatory diseases will grow, with 23.3 million deaths per year associated with heart dysfunction by 2030 and 32.3 million by 2050 [2]. Acute myocardial infarction (AMI) is the sudden reduction or blockage of blood flow, causing oxygen deficiency and myocardium damage [3]. The prevalence of AMI is high and accounts for over 270 daily admissions and costs the UK £9 billion annually [4,5]. Since severe irreversible damage predominantly occurs within two hours of symptom onset, early recognition and intervention are vital for AMI patient prognosis and resource management [6].

Due to the ambiguous nature of AMI symptoms, cardiac I troponin (cTnI) is the gold-standard AMI biomarker and the primary biomarkertest used to aid clinical decision-making, prioritise treatment, and discharge low-risk patients [6,7]. Cardiac troponin I levels exceeding 120 pg/mL indicates an AMI is likely occurring [8]. Cardiac troponin I levels begin to rise in early AMI, and the magnitude of this elevation is correlated with the risk of death, providing an incentive to detect cTnI for early identification and intervention [6].

Enzyme linked Immunosorbent Assays (ELISAs) are a primary cTnI determination method used but have limitations that impede rapid diagnosis needed for AMI [9,10]. Several other methods for cTnI detection are available including fluorescence immunoassay and surface plasmon resonance. (SPR) are used for cTnI determination, several generations of technology being developed with increasing sensitivity over time [10,11]. These traditional approaches are performed in a centralised laboratory by trained personnel with lengthy procedures and

* Corresponding author.
E-mail address: niamh.docherty@strath.ac.uk (N. Docherty).

https://doi.org/10.1016/j.sbsr.2024.100725
Received 1 October 2024; Received in revised form 16 December 2024; Accepted 19 December 2024
Available online 22 December 2024

large equipment, which delays diagnosis and contributes to emergency department backlogs [12]. Centralised laboratory testing can take more than 60 min compared to 20 min with point of care (POC) assays, an attractive alternative for cardiac troponin determination [13].

Literature has reported recent advancements in troponin POC detection including optical, test strips and microfluid paper based sensors which can detect picomolar concentration of cardiac troponin [14,15]. The advantages and limitations of each detection type are covered in several literature reviews [12,16,17]. Electrochemical immunosensors are of particular interest for cardiac troponin determination since this biosensing format combines the rapid detection capabilities of electrochemical measurements with the specificity of immunoassays by utilisation of the specific interaction between antigen and corresponding specific antibodies and the transduction of the product molecules into an electrochemical signal for antigen quantification [18,19]. Biosensor characteristics typically include high specificity, design simplicity, real-time responses, low sample volumes requirements with scope for integration and automation, which makes them compelling candidates for cTnI POC detection where both rapid and high sensitivity detection is necessary [12]. There is a wide range of materials used in biosensors, including metals and nanomaterials as substrate for target immobilisation and or electrochemical sensing. Gold based materials offer distinct advantages in electrochemical immunosensors by offering superior conductivity, exceptional biocompatibility for improved signal detection and stable biomolecule immobilisation. The chemical stability ensures reliable performance in diverse conditions and has efficient electron transfer pathways, enabling lower detection limits [20]. Furthermore, gold has flexible surface chemistry providing options for biomolecule immobilisation. These advantages paired with recent advancements that have simplified gold electrode fabrication, suggest gold electrodes are ideal electrochemical platforms for biosensing in low resource settings [21].

Many electrochemical immunosensors exploit the specificity of the sandwich ELISA approach to capture the antigen near the electrode surface (Fig. 1) [22]. Horseradish peroxidase (HRP) and 3,3′,5,5′-Tetramethylbenzidine (TMB) are commonly used as an enzymatic label and substrate pair in ELISAs [23]. HRP catalyses the oxidation of TMB, causing a colour change from colourless to blue. Due to the electroactive nature of TMB, chronoamperometry can be used to impose a voltage on the blue solution to induce oxidised TMB reduction. The magnitude of the current exhibited is an indirect measurement of antigen binding [23,24]. Glucose monitoring sensors are a prime example POC amperometric biosensors, and many estimate glucose levels by measuring the current generated by a redox mediator immobilised on the electrode surface [25].

Antibody immobilisation is a key consideration during sensor preparation for immunosensors [26,27]. Many immunosensors elect to attach the biorecognition element directly to the electrode surface that measures the electrochemical signal. Physical adsorption is a simple and low cost approach that relies on weak bonds such as Van Der Waals forces, hydrogen bonding or hydrophobic interactions to bind the capture entity to the electrode [28]. On gold surfaces, chemisorption uses a chemical crosslinker that exploits the strong affinity between thiol and gold to immobilise thiol-containing enzymes or antibodies on gold surfaces [27]. The immobilisation method can affect antibody orientation, loading, mobility and activity, attributes that affect biosensor sensitivity, specificity and stability [27].

Since the evolution of the glucose biosensor, there have been many advancements to measure smaller molecular targets that fluctuate in physiological disease states [22]. However, these novel sensors with complex materials, fabrication processes and high-sensitivity electrochemical techniques are often impractical in clinical use [19]. Thus, the remaining challenge for novel biosensor development for small molecular targets like cTnI is balancing cost, performance, and applicability [12]. Therefore, deliberately engineering simple but robust platforms may aid the translation of electrochemical biosensors into real-world applications.

Several electrochemical immunosensors have been developed for cardiac troponin I [16]. However, to our knowledge, a low-cost, simple, and portable electrochemical assay using off the shelf ELISA reagents has not been fabricated for cTnI detection. This paper introduces a low-cost, simple electrochemical immunosensor that repurposes ELISA antibodies and reagents. After antibody, reagent and electrode array characterisation, the ELISA protocol was adapted for electrochemical measurements. Optical ELISA product solution was transferred from a well plate to the thin gold film electrode with eight working electrodes (TGF-E8) for electrochemical detection of cTnI before antibody immobilisation methods were scrutinised for an electrochemical ELISA (EELISA) sensor. The study describes the formation of a physisorption and chemisorption sensor prototype for capture antibody immobilisation, with the latter employing sulfosuccinimidyl 6-(3′-(2-pyridyldithio) propionamido) hexanoate (sulfo-LC-SPDP) as a crosslinker to attach the capture antibody to the gold electrode surface. The performance of the two sensors is examined using calibrants in a buffer and diluted human serum. Finally, the sensors fabricated in this work were compared to recent cTnI electrochemical biosensors in the literature. The paper presents a significant advancement in developing a novel electrochemical immunosensor for cTnI detection, leveraging existing ELISA reagents and antibodies to create a practical, cost-effective, portable solution which is already operating within a clinically relevant detection range.

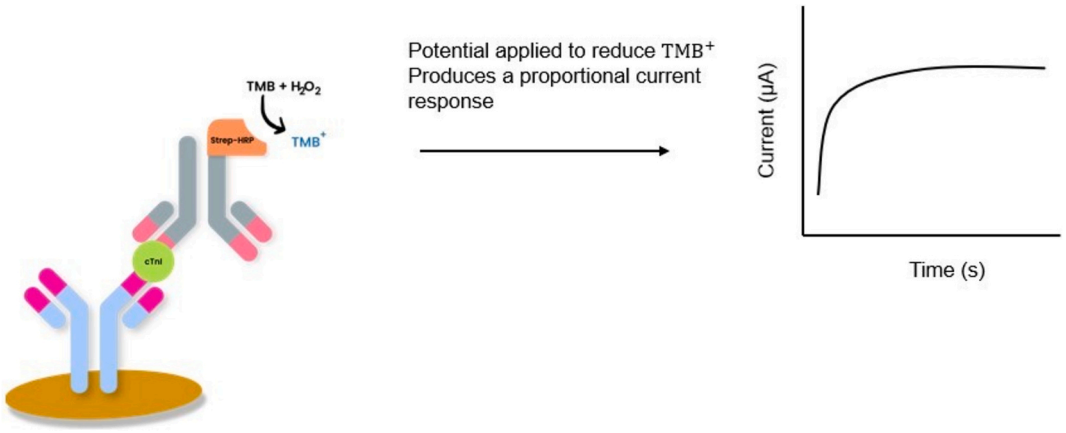

Fig. 1. A schematic of the electrochemical ELISA using HRP as an enzymatic label and TMB as the redox mediator with the current time transient recorded during measurement.

2. Materials and methods

2.1. Equipment

BioTek ELX800 Microplate reader, 400 to 750 nm, 6, 12, 24, 48, 96 well (Cole-Palmer, St Neots). Thin gold film electrode eight channel array (FlexMedical Solutions, Livingston). PalmSens4 Potentiostat (PalmSens, Netherlands). MUX8-R2 Multiplexer (PalmSens, Netherlands). Hitachi TM – 1000 microscope (Hitachi High-Tech Europe). Nanoscope IIIa (Digital Instruments, Santa Barbra California).

2.1.1. Chemicals and reagents

Cardiac troponin I ELISA kit (R&D systems, cat number DY6887–05) containing Human Troponin I Capture antibody (Part #844233), Human Troponin I Detection antibody (Part #844234), Human Troponin I Standard (Part #844235), Streptavidin-HRP B (Part #83975), Wash buffer 25 x concentrate (R&D Systems, WA126), ELISA Reagent diluent concentration 2 (R&D Systems, DY995), R&D systems matrix metalloproteinase-3 (MMP3) ELISA kit (R&D Systems, Cat. No. DY513), TMB Substrate Solution 1:1 mixture of Colour Reagent A (H_2O_2) and Colour Reagent B (Tetramethylbenzidine (TMB) (R&D Systems, Cat. No. DY999), H2SO4 (Sigma), Potassium Ferricyanide (Sigma), PBS (Sigma), 96-well plates (Sigma). cTnI depleted Human serum (Hytest, Cat. #8TFS2), C-reactive protein (CRP) (R&D Systems, DY1707), IL-6 (R&D systems, DY206), TNFα (R&D systems, DY210). All other reagents, including Phosphate-Buffered Saline (PBS) tablets, Bovine Serum Albumin (BSA) Solution (A7906), 1,4-dithiothreitol (DTT), 6-Mercapto-1-hexanol (MCH), and Sulfo-LC-SPDP (#803316) were purchased from Sigma Aldrich (UK).

2.1.2. Sensor fabrication

The thin gold film electrode arrays (TGF-E8) were manufactured by Flexmedical Solutions (Livingstone, UK). The sensor substrate was gold-spluttered polyester with a thickness on the Angstrom level, and the gold material was processed via laser ablation to produce a sensor with multiple measurement sites ($n = 8$). A reference sensor was printed using Ag/AgCl paste and dried using controlled forced air. The thickness of the Ag/AgCl reference electrode was in the 10–12 μm range. An optically clear insulator paste of 6–8 μm was screen printed onto the electrode array. Schematic of the TGF-E8 and photographs of the set up can be found in Supplementary Fig. 1 (Fig. S1).

2.1.3. Human serum preparation

Human serum was filtered through a 0.2 μm filter syringe, and 1 in 10 dilution was performed using reagent diluent. Diluted human serum was prepared as the diluent in cTnI standards (125–8000 pg/mL).

2.2. Experimental

A similar set up was used as photographed in Sánchez-Salcedo et al. work [29]. Electrochemical measurements were performed using a PalmSens PS4 Potentiostat driven by PSTrace 5.9 software (PalmSens, Houten, Netherlands). The TGF-E8s were connected to the potentiostat via an in-house custom eight-channel connector (Fig. S1) and a MUX-R2 multiplexer.

2.2.1. Electrode cleaning

Immediately before use, H_2SO_4 cycling was used to remove containments from the electrode surface and expose the gold electrode surface to improve electrode surface uniformity. The sample potential was cycled from 0 to 1.6 V (vs. Ag/AgCl) at a rate of 300 mV/s in 100 mM sulfuric acid on each working electrode until the scans were consistently overlapping. 12 scans were performed for electrodes used for characterisation; 16 scans were performed for electrodes prepped for electrochemical ELISAs.

2.2.2. Optical ELISA in plate format

A 96-well plate was coated with 2 μg/mL anti-human cTnI diluted in 1 % BSA in PBS (reagent diluent) and incubated overnight at room temperature. The wells were aspirated with 1× PBS three times, dried and blocked with reagent diluent for 1 h at room temperature. Washing removed excess reagent diluent, and cardiac troponin standards were prepared by serial dilution from 8000 to 125 pg/mL using reagent diluent. 8000 pg/mL of human MMP3 standard was prepared for the negative control. Each standard was incubated for 2 h at 25 °C ($n = 4$). To remove the cTnI solutions, washing was repeated before the biotinylated human troponin I detection antibody (400 ng/mL) was added to each well and incubated for 2 h at 25 °C. Streptavidin-HRP B was added to each well, and the plate was incubated in the dark for 20 min at room temperature. Substrate solution (1:1, TMB: H_2O_2) was added to each well, and the plate was incubated for 20 min in the dark. The enzymatic reaction was stopped with 100 mM H_2SO_4, and the optical density was measured at 450 nm.

2.2.3. Characterisation of TGF-E8

Clean electrodes were characterised by performing cyclic voltammetry (CV) between −0.2 V and 5 V and using 10 mM $K_3Fe[(CN)_6]$/$K_4[Fe(CN)_6]$ and scan rates of 100, 50, 25 and 10 mV/s. CV between −0.2 V and 0.5 V at 100 mV/s was performed on a clean TGF-E8 using various concentrations of $K_3Fe[(CN)_6]/K_4[Fe(CN)]_6$. to study the effect of redox mediator concentration on current. A linear fit was applied to the relationship between mean oxidation peak current and $K_3Fe[(CN)_6]$/$K_4[Fe(CN)]_6$ concentration. The square root of the scan rate and the mean oxidation peak current was also studied, a linear fit was applied and adjusted R^2 values were reported. TMB substrate solution and HRP (1:40) were cycled on a clean TGF-E8 from 0.0 V to 0.6 V, at a scan rate of 100 mV/s for each working electrode. Auto peak detection was utilised in PSTrace to find peak height and potential. The data were transferred to OriginPro for data analysis. Experimental details of scanning electron microscopy and atomic force microscopy can be found in the supplementary information (Fig. S3 and Fig. S4).

2.2.4. Electrochemical ELISA: Well to electrode

An optical ELISA was performed as described above. After TMB substrate solution incubation, the supernatant was transferred from the well plate to a cleaned TGF-E8. Chronoamperometry was performed at −0.2 V for 60 s with a 0.1 s time interval for each working electrode ($n = 8$).

2.2.5. Electrochemical ELISA: Physical adsorption sensor

Clean TGF-E8 working electrodes were covered with 12 μg/mL capture antibody and incubated overnight in a humidity chamber at 4 °C. The arrays were gently rinsed with 1× PBS and dried using controlled forced air. Each working electrode was covered with Superblock and the arrays were incubated for 15 min at room temperature. The working electrodes were rinsed and dried as before. The electrodes were covered with the standard solution and incubated at room temperature for 90 min. Washing was performed again, and detection antibody (800 ng/mL) was added to the electrode surface and incubated for 90 min at room temperature. The electrodes were washed and dried as before. The working electrode was covered with streptavidin-HRP B and incubated for 20 min in the dark at room temperature. All electrodes were washed and dried before adding ELISA substrate solution (TMB: H_2O_2) for a 20 min incubation at room temperature in the dark. Chronoamperometry was performed at −0.2 V for 60 s with a 0.1 s time interval.

2.2.6. Electrochemical ELISA: Chemisorption sensor

The capture antibody thiolation approach was adapted from previous literature (Fig. 2) [30]. A 2:1 solution of 200 μg/mL capture Ab in 5× PBS and aqueous sulfo-LC-SPDP solution (40 mM) was prepared and shaken vigorously (350 rpm) for 1 h. An equal volume of DTT solution

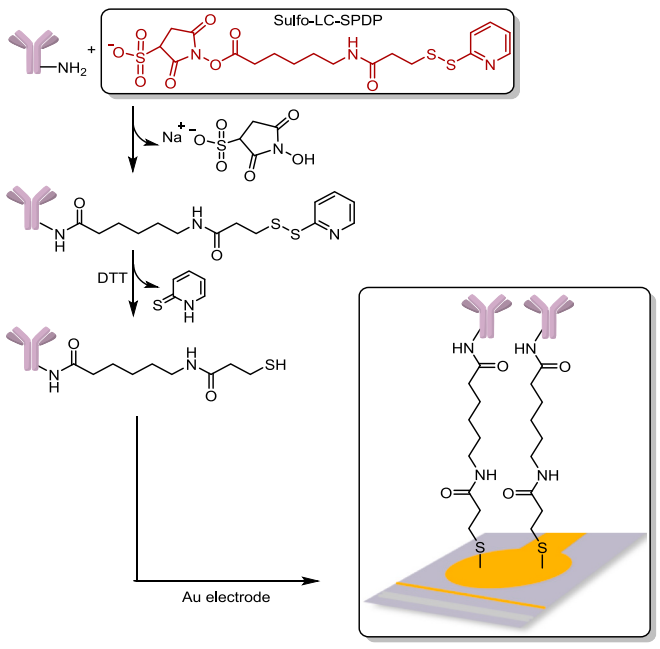

Fig. 2. Capture antibody Immobilisation using a sulfosuccinimidyl 6-(3′-(2-pyridyldithio) propionamido) hexanoate as a crosslinker to create a S—Au bond between the antibody and electrode.

(150 mM in 5× PBS) was added to the mixture and left to react for 45 min to break thiolated disulphide bonds. The thiolated antibody solution was dropped onto the working electrode and left inside a humidity chamber overnight at 4 °C. TGF-E8s were rinsed with 1× PBS. Electrode surfaces were blocked with 1 mM MCH in 1× PBS for 30 min, followed by two applications of 1× PBS for 10 min and rinsed. After electrode functionalisation, cTnI (125–8000 pg/mL) and MMP3 (8000 pg/mL) standards resuspended in reagent diluent, or 10 % human serum, were added to the sensors followed by a 90 min incubation at 25 °C. Electrodes were rinsed as before, and detection antibody (800 ng/mL) was added to the sensors for a 90 min incubation at 25 °C. Streptavidin-HRP B was added to the working electrodes before 20 min incubation at 25 °C. The electrode was rinsed, and TMB substrate solution was added to coat the sensor electrodes for a 20 min incubation at 25 °C before chronoamperometry measurements were taken at −0.2 V for 45 s.

2.2.7. Theory and calculation

Electrochemical data was transferred from PSTrace to Origin Pro for analysis. Optical data was also analysed in Origin Pro. For optical and amperometric ELISA experiments, the data were log transformed and respective mean and standard deviations calculated. The mean steady state current was defined as the current exhibited at 45 s ($n = 8$). For most datasets, a four parameter logistics (4PL) fit was used to represent the relationship between the log of cTnI concentration and optical density or mean steady state current. The detection limit was defined as the mean + 3 SD of the log optical density or steady state current for the negative control. This value was then plugged into the 4PL equation to determine the limit of detection (LOD) regarding cTnI concentration. Where y is the response (optical density or current), a is the maximum value, d is the minimum value, x is the EC_{50} concentration, b is the gradient and c is the analyte concentration. The adjusted R^2-value was reported for each analysis.

$$y = \frac{a-d}{1+\left(x/c\right)^{b}} + d \tag{1}$$

Eq. (1) 4-parameter logistic equation used for dose response curves interpretation.

For visualisation of optical and electrochemical ELISA experiments, the logged data was plotted, and the x-axis labels were adjusted to show the linear concentration values in pg/mL.

AFM data was analysed using WxSM5.0 Develop 10.3 [31] to find the height, amplitude and the root mean square error value to characterise the roughness of the TGF-E8 working electrodes.

2.2.8. Specificity and reproducibility

Please refer to supporting information for details on the specificity and reproducibility studies for chemisorption functionalised TGF-E8s.

3. Results and discussion

3.1. Benchmarking performance of the optical ELISA and characterisation of TGF-E8

Before developing a biosensor system, conventional ELISA measurements were performed to benchmark the immunoassay reagent and antibody sensitivity. A linear fit was most representative for the cTnI ELISA in buffer (Adjusted $R^2 = 0.995$), with a LOD of 159 pg/mL, which is higher than the stated working range (125–8000 pg/mL) (Fig. 3.A). When performed in 10 % human serum, the LOD was lower at 84.5 pg/mL (Adjusted $R^2 = 0.974$) (Fig. 3.B), likely due to the cTnI or complex proteins in the human serum causing non-specific binding. Variation between samples also increased, demonstrated by the increase in standard deviation (Fig. 3.B), suggesting the antibody performance is diminished in more complex samples.

Next, the underlying multiplexed gold sensor was developed and characterised. The thin gold film arrays have been characterised and modified using a sulfur thiol bond in previous literature [29]. Cyclic voltammetry is a standard electrochemical technique used to analyse redox reaction near the electrode surface or as a cleaning process [32]. Sulfuric acid cycling was used as more rough cleaning methods such as piranha cleaning can damage the electrode surface, whereas CV cycling in sulfuric acid the removes surface containments without damaging the gold [33]. The CV was repeated on each electrode until the gold oxide reduction peak no longer increased in size (Fig. S2). 16 scans were implemented for each working electrode used for electrochemical ELISA purposes for consistency. TGF-E8 characterisation was performed by studying the effect of scan rate using 10 mM $K_3Fe[(CN)_6]/K_4[Fe(CN)_6]$ solution (Fig. 3.C). The TGF-E8 were affordable (£4.85 per unit), and the peak separation ~120 mV, was higher than the ideal 59 mV, but suggested adequate electron transfer to allow the reversible redox reaction to occur [32]. The mean peak oxidation current increased linearly with the square root of the scan rate (Adjusted $R^2 = 0.999$) (Fig. 3D), suggesting the reaction is limited by the diffusion of electroactive species to the electrode surface [32]. TGF-E8 characterisation was performed by studying the effect of scan rate using 10 mM $K_3Fe[(CN)_6]/K_4[Fe(CN)c_6]$ solution (Fig. 3.E) and there was a linear relationship between oxidation peak height and $K_3Fe[(CN)_6]/K_4[Fe(CN)c_6]$ concentration (Adjusted $R^2 = 0.999$) (Fig. 3.F). Previous studies have used HRP as a label and TMB as the redox mediator to detect cTnI electrochemically [24]. The reduction of TMB^+ was studied by performing CV on the TMB substrate solution on the TGF-E8 surfaces. Fig. 3.G shows TMB^+ and TMB^{2+} reduction at 0.145 V and 0.288 V, respectively. Since the TMB^+ reduction exhibited a larger peak height and current magnitude, TMB^+ was selected as the redox reporter via chronoamperometry with an electrode biased at −0.2 V.

Scanning Electron Microscopy was also performed on the working electrodes to determine if the causes of this variability were apparent; details of this analysis are available in the supporting information (Fig. S3). The topography of the TGF-E8 working electrode was characterised using atomic force microscopy. A 20 × 20 μm scan revealed variations in surface height, with certain regions displaying elevations higher than others (Fig. S4). The root mean square error value, calculated as a measure of surface roughness, was determined to be 122.34

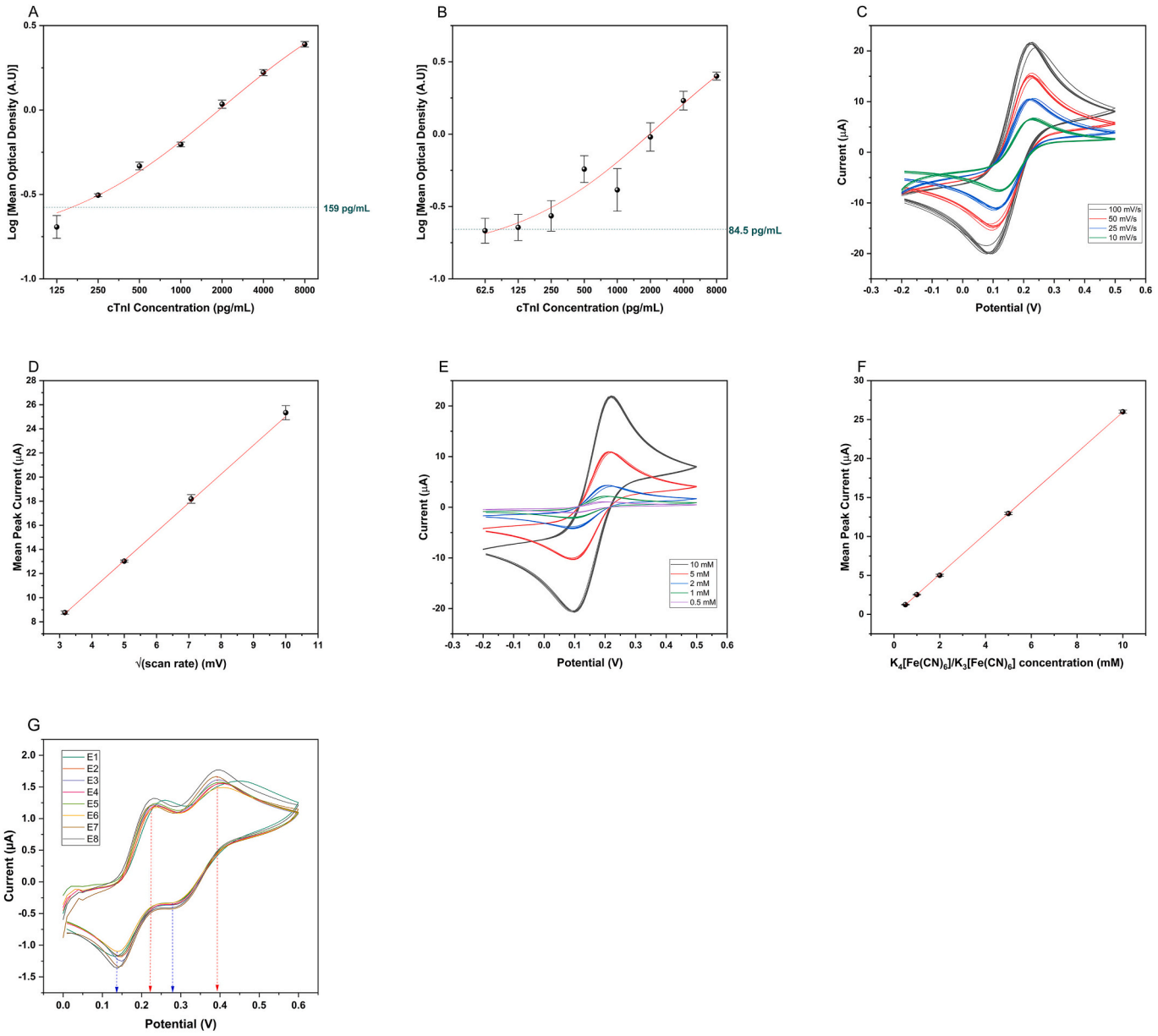

Fig. 3. Characterisation of the ELISA reagents and TGF-E8. A) Dose response curve with cTnI standards (1258000 pg/mL) reconstituted in reagent diluent and B) in 10 % human serum. Dots and error bar represent mean log optical density ± one standard deviation for each cTnI standard (n=4). LOD concentration value (cyan dashed line) was found using the 4PL (red line). C) CV of $K_3[Fe(CN)_6]/K_4[Fe(CN)_6]$ at various scan rates. D) Scatter plot with a linear relationship of the square root of the scan rate and mean peak current. E) Cyclic voltammetry of varying $K_3[Fe(CN)_6]/K_4[Fe(CN)_6]$ concentrations from 0.5 to 10 mM. F) Scatter plot of $K_3[Fe(CN)_6]/K_4[Fe(CN)_6]$ concentration versus mean peak current. G) CV of TMB substrate solution (1:1 TMB: H_2O_2) on each electrode (E1- E8) of the TGF-E8. Peak potentials are highlighted by blue (reduction) and red (oxidation) arrows. (For interpretation of the references to colour in this figure legend, the reader is referred to the web version of this article.)

nm. These findings highlight non-uniformity across the electrode surface, which may influence its electrochemical performance. While the presence of 'pinholes' in the otherwise uniform gold surface is concerning, their effect on overall electrode performance seems to be minimal, with no presence of the underlying substrate being visible in CV measurements. What is potentially of more concern is the poor definition of working electrode areas seen which will inevitably lead to variability in results, highlighted by the lack of a sharp edge seen in the boundary between the electrode area and surrounding dielectric.

3.2. Transition from optical to electrochemical cTnI detection

After characterising the optical ELISA reagents and the electrochemical properties of the TGF-E8, comparing the amperometric detection of cTnI with the traditional optical methods was necessary. The absorbance ELISA is a gold standard method for cTnI determination and was used as a comparison to amperometric cTnI detection. Optical ELISA and EELISA in plate format were performed in parallel, and a similar trend was observed between optical and electrochemical data in this setup (Fig. 4.A). The EELISA exhibited a dose dependent response with a LOD of 1000 pg/mL (Adjusted $R^2 = 0.999$) (Fig. 4.B). The optical ELISA LOD was 349 pg/mL (Fig. S5), indicating that using ELISA supernatant for amperometric cTnI detection was less effective. Notably, the optical ELISA LOD is inferior to previous optical ELISA experiments, indicating less oxidised TMB production or non-specific binding in the negative control. It can be assumed that the commercial supplier

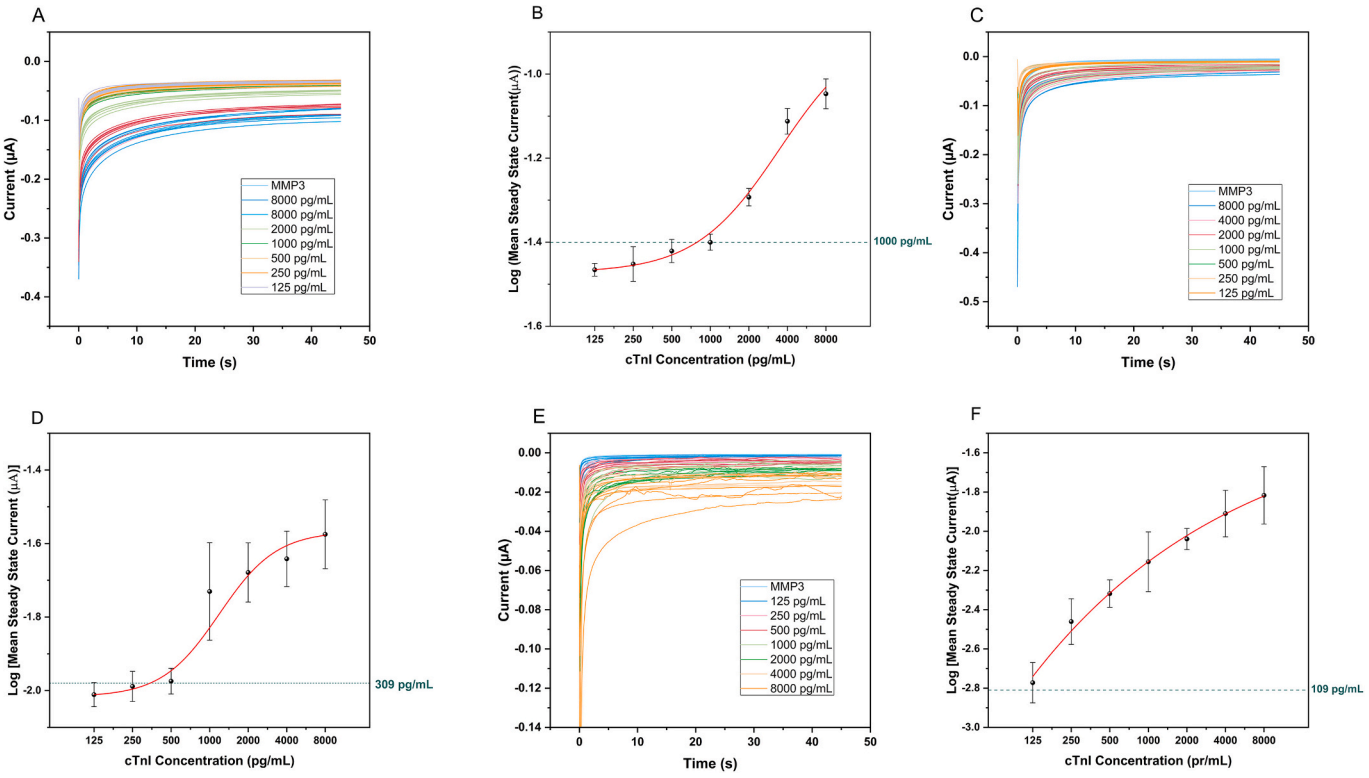

Fig. 4. The amperometric detection of cTnI using TGF-E8s. A) Current time transients obtained after transferring ELISA product solution from plate to TGF-E8s. B) Dose response curve of mean steady state current and cTnI concentration in the well to plate electrochemical ELISA ($n = 8$). C) Physisorption EELISA current transient graph. D) Dose response curve after physisorption sensor EELISA. E) Dose response curve of mean steady state current and cTnI concentration (n = 8). E) The current transient graph for the chemisorption sensor EELISA. F) Dose response curve after chemisorption EELISA. 8000 pg/mL MMP3 was used as a control for each assay. The dashed line in teal colour indicates LOD concentration value. (For interpretation of the references to colour in this figure legend, the reader is referred to the web version of this article.)

optimised the ELISA reagents and antibodies for their intended purpose, so the dose response curve obtained with these affordable antibodies was promising for further sensor development. The lower sensitivity of the electrochemical detection approach is likely due to the comparatively long distance between electroactive TMB^+ in bulk solution. Product diffusion occurs in all directions, including away from the electrode surface, increasing the distance between the surface and the electroactive product of interest and resulting in a smaller steady state current [34]. It was hypothesised that greater sensitivity may be achievable by chemically crosslinking the sandwich immunocomplex to the electrode and decreasing the distance between TMB^+ and the electrode surface.

3.3. Electrochemical ELISA on TGF-E8s via physisorption of the capture antibody

Once confirmed that the TGF-E8 sensors could detect oxidised TMB in the product solution, capture antibody physisorption was examined to determine whether the immunocomplex could be successfully assembled on the sensor surface. Fig. 4.C shows the current time transients exhibited. The physisorption sensor displayed a dose dependent response with a good 4PL fit (Adjusted $R^2 = 0.996$) with a LOD calculated from the 4PL fit to be 309 pg/mL (Fig. 4.D). It was hypothesised that unpredictable antibody orientation and spacing occurred when using physical adsorption, which resulted in the variation in antigen binding and steady state current between working electrodes as shown by the large error bars in Fig. 4.D [26]. A second sensor variant was constructed using a semi-covalent immobilisation approach to ensure proper antibody immobilisation and enhance the probability of antibody-antigen interactions.

Minor adjustments to the commercial ELISA protocol were made to enhance immunocomplex construction on the electrode surface. The use of Superblock for passivation of the bare gold electrode after capture antibody incubation reduced incubation time and non-specific binding (Fig. S6). There is scope to reduce the incubation time further, and other incubation periods could be optimised to reduce fabrication and assay time [35].

3.4. Electrochemical ELISA via chemisorption of capture antibody using Sulfo-LC-SPDP

The crosslinker has been used for many detection platforms to promote more efficient orientation and stability via self-assembled monolayer formation that used semi-covalent linkage between thiol groups on the biorecognition element and the gold transducer surface [27,30,36,37]. Current time transients showed that as cTnI concentration increased, the steady state current increased (Fig. 4.E). The noise observed in Fig. 4.E was likely due to an incorrect connector position for optimal contact. The LOD calculated was 109 pg/mL (Adjusted $R^2 = 0.999$), lower than the physisorption sensor (309 pg/mL) (Fig. 4.F), indicating that chemisorption using the crosslinker improved capture antibody immobilisation. With promising results, the sensors were examined with diluted human serum to determine the impact of more complex samples on sensor performance.

3.5. Performance of sensors in human serum

The mean steady state current and total current produced was highest at 8000 pg/mL cTnI and generally decreased as cTnI concentration decreased for both sensors. The steady state reached appeared

more consistent for the chemisorption system (Fig. 5A and C). Once again, showing that greater control of the capture antibody immobilisation appeared to reduce variation between electrodes on the TGF-E8s as hypothesised. Physisorption has benefits, including cost-effectiveness, simplicity and minimal impact on enzyme activity. However, as mentioned, physisorption is a reversible process, and desorption and non-specific adsorption can occur throughout sensor fabrication or measurement, resulting in poor reproducibility, particularly in more complex samples [18,26]. The physisorption sensor exhibited a lower LOD of 233 pg/mL (Adjusted $R^2 = 0.999$) (Fig. 5.B) when the EELISA was performed using cTnI standards in diluted serum compared to the proprietary 'Reagent Diluent' supplied with the kit (309 pg/mL) (Fig. 4. D). Conversely, the chemisorption-based sensor sensitivity slightly decreased rin serum with a LOD of 130 pg/mL indicating further work is needed to overcome the effect of serum on the amperometric signal (Adjusted $R^2 = 0.999$) (Fig. 5.D). Error bars in Fig. 5B and D indicate that variation was lower for the chemisorption approach, yet large variability was exhibited by the array challenged with 2000 pg/mL, due to an outlier on channel 1 (Fig. S7). The cTnI intrinsically present in the human serum should have a negligible effect since serum from healthy individuals was used and diluted. It is hypothesised that the decrease in sensitivity is likely due to proteolysis of free form cTnI in the diluted human serum, preventing the antibody capture and recognition. Also, cTnI primarily exists in the more stable binary or ternary form (cTnIC/cTnITC) in blood, which would give a better representation of troponin in a clinical sample [38,39]..

The specificity and reproducibility of the chemisorption sensor was evaluated in 10 % human serum (Fig. S8). IL-6, CRP and TNFα were used to determine the specificity of the sensor. A distinguishable signal was exhibited for sensors challenged with cTnI (8000 and 100 pg/mL) compared to sensors challenged with 8000 or 250 pg/mL of the negative controls, demonstrating the sensor's specificity. Reproducibility was also demonstrated but outliers of 1 working electrode on the array caused an increase in variation for arrays 4, 6 and 7 (Fig. S8·B). When outliers were not present, the coefficient of variation was below 18.7 % for each array. It is hypothesised that the introduction of microfluidics and flow cells could minimise the variation in immobilisation between working electrodes and therefore the output signal [40].

3.6. Comparison of sensors to novel Immunosensors in literature

The performance of TGF-E8 immunosensors fabricated in this study

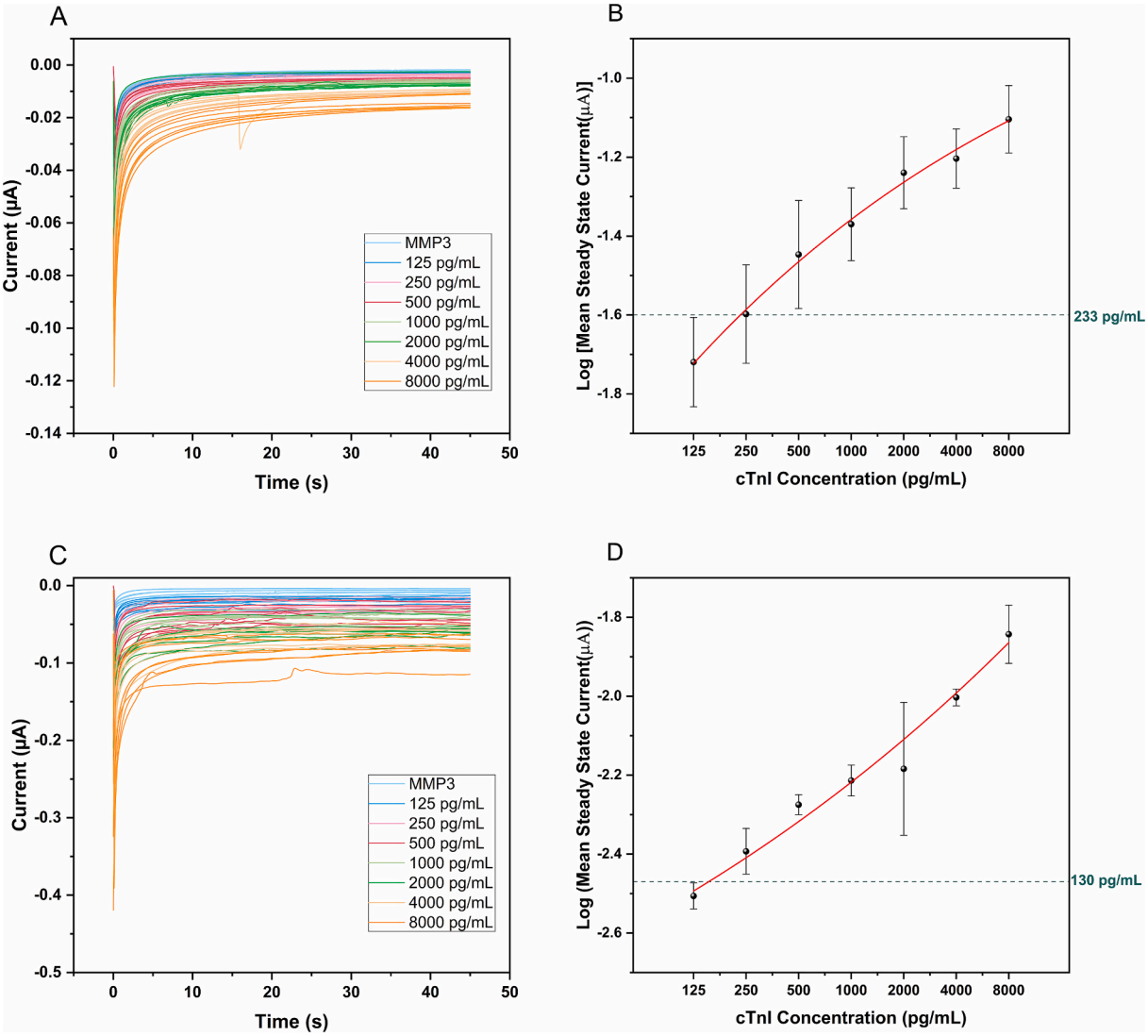

Fig. 5. Performance of TGF-E8 cTnI sensors in 10 % Human Serum. A) Current-time transients for physisorption sensor B) 4PL fit for physisorption sensor. C) Current-time transient for chemisorption sensor. D) 4PL fit for chemisorption sensor. Concentration LOD of each sensor in human serum displayed by cyan dashed line and labelled. (For interpretation of the references to colour in this figure legend, the reader is referred to the web version of this article.)

Table 1
Electrochemical Immunosensors for cardiac troponin I detection.

Biosensor	Assay Principle	Linear Range	Detection Limit	Reference
Ab-HRP/cTnI/Ab/superblock/TGF-E8	CA	N/A	233 pg/mL	This work
Ab-HRP/cTnI/Ab/Sulfo-LC-SPDP/MCH/TGF-E8	CA	N/A	130 pg/mL	This work
Apt-HRP/cTnI/Apt-CES-GO/SPE	CA	1–10 pg/mL	0.6 pg/mL	[41]
cTnI/BSA/Ab/Pt/Au–B,S,N-rGO/GCE	CA	0.1 pg/mL-50 ng/mL	0.082 pg/mL	[43]
PtPdCu/BNC/Ab2/cTnI/BSA/Ab1/Au@SNHC/GCE	CA	10 fg/mL–100 ng/mL	4.27 fg/mL	[44]
Ab/p-COFs/p-SiNWs/cTnI	PEC	5 pg/mL to 10 ng/mL	1.36 pg/mL	[47]
cTnI/BSA/Apt/MCH/AuLSGE	DPV	N/A	2.58 ng/mL	[48]
glycine/ab-cTnI/AuNPs–PAH/LC_{col}/GCE	LSV, EIS	0.01 to 0.3 ng/mL	0.005 ng/mL (LSV) and 0.01 ng/mL (EIS)	[52]
anti-cTnI Ab/AuNPs@GQDs/SPGE	SWV, CV, EIS and CA	1 to 1000 pg/mL	0.1 pg/mL (buffer) and 0.5 pg/mL (serum)	[54]

Ab: Antibody; Ab1: Primary Antibody; Ab2: Secondary Antibody; Ab-HRP: Horseradish Peroxidase-Conjugated Antibody; Apt-HRP: Horseradish Peroxidase-Conjugated Aptamer; Apt-CES-GO: Aptamer-Carboxymethlsilentriol Graphene Oxide; AuNPs@GQDs: Gold Nanoparticles modified with gold quantum dots; Au@SNHC: Gold Nanoparticles Modified with Sulfur Nitrogen Co-Doped Hollow Porous Carbon; AuNPs–PAH: gold nanoparticles stabilized in polyallylamine hydrochloride; BNC: Boron Nitrogen Double-Doped Carbon; BSA: Bovine Serum Albumin; cTnI: Cardiac Troponin I; CuFe2O4-Pd-Ab2: CuFe2O4-Pd Nanoparticles with Secondary Antibody; *E*-Au: Electrochemical Gold Substrate; GCE: Glassy Carbon Electrode; LCcol: columnar liquid crystal; MCH: 6-Mercapto-1-hexanol; Pt/Au–B,S,N-rGO: Platinum/Gold Boron, Sulfur, and Nitrogen Doped Reduced Graphene Oxide; PEC:Photoelectrochemical PtPdCu/BNC: Platinum Palladium Copper with Boron Nitrogen Double-Doped Carbon; p-COFs; Porphyrin Covalent Organic Framework; p-SiNWs: p-type silicon nanowire arrays; SPE: Screen-Printed Electrode; SPGE: Scree-printed gold electrode; Sulfo-LC-SPDP: sulfosuccinimidyl 6-(3′-(2-pyridyldithio)propionamido)hexanoate; TGF-E8: Thin Gold Film Electrode.

and recent cTnI immunosensors are detailed in Table 1 for comparison. Superior analytical performance is often achieved utilising complex materials and nanocomposites to enhance target binding, conductivity and electron transfer [41–47]. However, the sensors in this work outperformed some iterations with more advanced configurations [48]. More sensitive electroanalytical techniques, such as DPV [49], SWV [50,51], LSV or EIS [52], are implemented in high-sensitivity cTnI platforms but can face more translatability issues due to their sensitivity in less controlled environments such as POC settings. Highly sensitive electrochemical measurements and complex signal amplification strategies involving complex fabrication processes can achieve impressive cTnI sensitivity. Nevertheless, these systems can be resource-intensive, expensive, and pose scalability manufacturing challenges. For instance, the systems outlined in Table 1, reach the sensitivity required but would be challenging to implement for some healthcare systems due to cost. Stability and specificity are often examined but, long-term stability, operational complexity and sensitivity to environmental conditions are not clearly discussed but are critical for use in diverse POC environments [53]. Mansuriya et al. developed an immunosensor capable of a similar sensitivity (1 pg/mL to 1000 pg/mL) using four different analytical techniques, suggesting comparable analytical performance can be obtained across electroanalytical methods despite inherent differences in sensitivity [54]. The sensors herein also outperform many graphene based and aptamer based cTnI sensors, including Beduk et al.'s multiplex sensor made from laser-scribed graphene (LSG) modified with electrochemically deposited gold nanoparticles, functionalized with thiol-modified aptamers specific to cardiac troponin I (cTnI), resulting in sensitivity of 2.58 ng/mL [48]. Thus, a simple, robust amperometric biosensor that utilises the advantages of gold electrodes, Immunoassay technology and electrochemical detection sensitivity such as the sensor herein could be the breakthrough required for point-of-care cTnI determination with further adaptations to improve system sensitivity. The portable sensor would be ideal for pre-hospital or emergency department cTnI tests and multiple measurements could occur concurrently on a single array. The absence of nanomaterials and a simple assay procedure would allow clinical staff to use this device in diverse POC environments. Therefore, while the systems in this work are not as sensitive as other sensors in the research domain, it is close to being relevant for clinical purposes since 120 pg/mL is the cut off for a myocardial infarction to be likely [8].

3.7. Comparison of sensors to state-of-the-art cTnI POC devices

Along with sensitivity, stability, user-friendliness and specificity, one of the main requirements for POC diagnostics is affordability, and the main hurdle in POC diagnostics is balancing the requirements [53]. Table 2 examines the cost of the sensors herein and competitors currently on the market. The figures in Table 2 are indicative estimates, subject to change, and require a supplier liaison for precise quotes. Costs of goods of the sensors in this work would decrease with scaled-up production to reduce the true device and strip cost. Table 2 indicates that the current costs of goods are more affordable than several tests with a similar sensitivity range. In Table 2, the cost device for this work was selected as a PalmSens Pico Stat, which is appropriate for POC device integration and affordable and compatible with the system's desired features.

3.8. Future work

The work in this study should inform future work to create a more sensitive cTnI electrochemical immunosensor while maintaining the comprehensive elements of the sensor. Even though the affordable ELISA reagents and antibodies were successfully transferred to the electrochemical assay, different antibody parings with known target epitopes should be explored to maximise binding efficiency [55,56]. Further characterisation of the electrode and antibody immobilisation would provide great insight into the orientation and packing of the antibodies on the electrode surface. Further adjustments that would improve analytical performance without compromising practicality should be examined. The lack of sensitivity in diluted human serum may be due to the instability of free form cTnI in real samples [38,39]. Additional studies should spike cardiac troponin depleted serum with cTnIC or cTnITC complex or use clinical samples with elevated troponin levels to negate the possibility of cTnI instability affecting the response exhibited. The introduction of microfluidics into the system would further tackle the variability observed between working electrode outputs by allowing uniform functionalisation of each electrode [40].

Table 2
Estimated cost comparison between this work and state-of-the-art cTnI POC devices.

Product	Device Cost ($)	Strip Cost ($)
Abbot iSTAT	8 K	14
Quidell/Alere Triage	8 K	38
Roche Cardiac POC troponin	2.5 K	40
Siemens CS Stratus	35 K	8.5
This work	535*	12

* Cost of goods.

4. Conclusions

Off the shelf ELISA reagents were used to construct a cTnI electrochemical immunosensor. The chemisorption sensor demonstrated greater sensitivity than the benchmark ELISA when challenged with cTnI standards in buffer. The devices fabricated and tested herein were found to be approaching clinically relevant concentrations of cTnI for AMI cases with similar analytical power to the absorbance-based ELISA. Detection limits of 233 pg/mL and 130 pg/mL were found for the physisorption and chemisorption sensor variants when tested with diluted human serum spiked with cTnI. The performance of the sensors was compared to the literature, and the sensors approach high sensitivity levels with a simple and more affordable set-up than more advanced cTnI sensors. This platform is the first step to a robust and straightforward cTnI immunosensor. With further advancements such as reducing sample to result time, using sophisticated antibodies and reagents, and integrating the antibodies and reagents into a singular platform, the low cost and portable sensor could deliver sensitive cTnI detection in POC settings.

Author contributions statement

Authorship contributions are tracked using the appropriate CRediT system categories: conceptualisation – DC (equal), ND (equal): data curation – ND (lead), LC (supporting), SM (supporting); formal analysis – ND (lead), LC (supporting); funding acquisition- DC (lead); investigation- ND (equal), LC (equal); methodology- DC (equal), ND (equal); project administration- ND (lead); resources- DC (lead); supervision- DC (lead), SP (supporting), YF (supporting); visualisation- ND (lead), LC (supporting); writing- ND (lead), DC (supporting); review & editing- ND, LC, SP, YF, SM, DC (equal).

Declaration of competing interest

There are no conflicts to declare.

Data availability

Data is available at doi:10.15129/784b5d11-1fc4-42b2-b922-c64eee5c2e7b.

Acknowledgements

The authors acknowledge and are grateful to the Advanced Diagnostics Centre at the University of Strathclyde, which facilitates their collaboration. ND Thanks NML hosted at LGC and the University of Strathclyde for studentship funding. SM thanks the EPSRC Doctoral Training Partnership EP/T517938/1 for his scholarship. DC thanks British Heart Foundation for funding through a Translation Award (TA/F/23/210048). All authors thank Dr. Fraser Gunn for his training on AFM usage.

Appendix A. Supplementary data

Supplementary data to this article can be found online at https://doi.org/10.1016/j.sbsr.2024.100725.

Notes and references

[1] Cardiovascular Diseases (CVDs). https://www.who.int/news-room/fact-sheets/detail/cardiovascular-diseases-(cvds, 2024 (accessed September 25, 2024).
[2] World Heart Federation (Ed.), Four paths to better cardiovascular health: World Heart Vision 2030, 2024. https://world-heart-federation.org/news/four-paths-to-better-cardiovascular-health-world-heart-vision-2030/ (accessed April 11, 2024).
[3] Fourth Universal Definition of Myocardial Infarction (2018) | Circulation, 2024, https://doi.org/10.1161/CIR.0000000000000617 (accessed May 21, 2024).
[4] UK Hospital Statistics, NHS Digital/Public Health Scotland/NHS Wales/DH Northern Ireland, 2024.
[5] BHF analysis of OHID (England) ONS Nomis (Wales), NRS (Scotland) and NISRA 2018–20 Mortality Data, 2024.
[6] P. Garg, P. Morris, A.L. Fazlanie, S. Vijayan, B. Dancso, A.G. Dastidar, S. Plein, C. Mueller, P. Haaf, Cardiac biomarkers of acute coronary syndrome: from history to high-sensitivity cardiac troponin, Intern. Emerg. Med. 12 (2017) 147–155, https://doi.org/10.1007/s11739-017-1612-1.
[7] J.-P. Collet, H. Thiele, E. Barbato, O. Barthélémy, J. Bauersachs, D.L. Bhatt, P. Dendale, M. Dorobantu, T. Edvardsen, T. Folliguet, C.P. Gale, M. Gilard, A. Jobs, P. Jüni, E. Lambrinou, B.S. Lewis, J. Mehilli, E. Meliga, B. Merkely, C. Mueller, M. Roffi, F.H. Rutten, D. Sibbing, G.C.M. Siontis, ESC Scientific Document Group, A. Kastrati, M.A. Mamas, V. Aboyans, D.J. Angiolillo, H. Bueno, R. Bugiardini, R. A. Byrne, S. Castelletti, A. Chieffo, V. Cornelissen, F. Crea, V. Delgado, H. Drexel, M. Gierlotka, S. Halvorsen, K.H. Haugaa, E.A. Jankowska, H.A. Katus, T. Kinnaird, J. Kluin, V. Kunadian, U. Landmesser, C. Leclercq, M. Lettino, L. Meinila, D. Mylotte, G. Ndrepepa, E. Omerovic, R.F.E. Pedretti, S.E. Petersen, A.S. Petronio, G. Pontone, B.A. Popescu, T. Potpara, K.K. Ray, F. Luciano, D.J. Richter, E. Shlyakhto, I.A. Simpson, M. Sousa-Uva, R.F. Storey, R.M. Touyz, M. Valgimigli, P. Vranckx, R.W. Yeh, E. Barbato, O. Barthélémy, J. Bauersachs, D.L. Bhatt, P. Dendale, M. Dorobantu, T. Edvardsen, T. Folliguet, C.P. Gale, M. Gilard, A. Jobs, P. Jüni, E. Lambrinou, B.S. Lewis, J. Mehilli, E. Meliga, B. Merkely, C. Mueller, M. Roffi, F.H. Rutten, D. Sibbing, G.C.M. Siontis, ESC guidelines for the management of acute coronary syndromes in patients presenting without persistent ST-segment elevation, Eur. Heart J. 42 (2021) (2020) 1289–1367, https://doi.org/10.1093/eurheartj/ehaa575.
[8] High Sensitivity Troponin I, South Tees Hospitals NHS Foundation Trust. https://www.southtees.nhs.uk/services/pathology/tests/high-sensitivity-troponin-i/, 2022 (accessed December 2, 2024).
[9] S. Aydin, K. Ugur, S. Aydin, İ. Sahin, M. Yardim, Biomarkers in acute myocardial infarction: current perspectives, Vasc. Health Risk Manag. 15 (2019) 1–10, https://doi.org/10.2147/VHRM.S166157.
[10] Z. Yuan, L. Wang, J. Chen, W. Su, A. Li, G. Su, P. Liu, X. Zhou, Electrochemical strategies for the detection of cTnI, Analyst 146 (2021) 5474–5495, https://doi.org/10.1039/D1AN00808K.
[11] I. Gokhan, W. Dong, D. Grubman, K. Mezue, D. Yang, Y. Wang, P.U. Gandhi, J. M. Kwan, J.-R. Hu, Clinical biochemistry of serum troponin, Diagnostics 14 (2024) 378, https://doi.org/10.3390/diagnostics14040378.
[12] A. Campu, I. Muresan, A.-M. Craciun, S. Cainap, S. Astilean, M. Focsan, Cardiac troponin biosensor designs: current developments and remaining challenges, Int. J. Mol. Sci. 23 (2022) 7728, https://doi.org/10.3390/ijms23147728.
[13] P. Collinson, Cardiac troponin by point-of-care testing: the once and future king?*, J. Am. Coll. Cardiol. 75 (2020) 1125–1127, https://doi.org/10.1016/j.jacc.2019.12.064.
[14] H. Fu, Z. Qin, X. Li, Y. Pan, H. Xu, P. Pan, P. Song, X. Liu, Paper-based all-in-one origami Nanobiosensor for point-of-care detection of cardiac protein markers in whole blood, ACS Sens. (2023), https://doi.org/10.1021/acssensors.3c01221.
[15] S. Bayoumy, I. Martiskainen, T. Heikkilä, C. Rautanen, P. Hedberg, H. Hyytiä, S. Wittfooth, K. Pettersson, Sensitive and quantitative detection of cardiac troponin I with upconverting nanoparticle lateral flow test with minimized interference, Sci. Rep. 11 (2021) 18698, https://doi.org/10.1038/s41598-021-98199-y.
[16] R.D. Crapnell, N.C. Dempsey, E. Sigley, A. Tridente, C.E. Banks, Electroanalytical point-of-care detection of gold standard and emerging cardiac biomarkers for stratification and monitoring in intensive care medicine - a review, Microchim. Acta 189 (2022) 142, https://doi.org/10.1007/s00604-022-05186-9.
[17] A.I. Saviñon-Flores, F. Saviñon-Flores, G. Trejo, E. Méndez, Ş. Ţălu, M.A. González-Fuentes, A. Méndez-Albores, A review of cardiac troponin I detection by surface enhanced Raman spectroscopy: under the spotlight of point-of-care testing, Front. Chem. 10 (2022), https://doi.org/10.3389/fchem.2022.1017305 (accessed January 17, 2024).
[18] J.E. Contreras-Naranjo, O. Aguilar, Suppressing non-specific binding of proteins onto electrode surfaces in the development of electrochemical Immunosensors, Biosensors 9 (2019) 15, https://doi.org/10.3390/bios9010015.
[19] F. Mollarasouli, S. Kurbanoglu, S.A. Ozkan, The role of electrochemical Immunosensors in clinical analysis, Biosensors (Basel) 9 (2019) 86, https://doi.org/10.3390/bios9030086.
[20] T. Jamshidnejad-Tosaramandani, S. Kashanian, K. Omidfar, H. Schiöth, Recent advances in gold nanostructure-based biosensors in detecting diabetes biomarkers, Front. Bioeng. Biotechnol. 12 (2024) 1446355, https://doi.org/10.3389/fbioe.2024.1446355.
[21] M. Zamani, V. Yang, L. Maziashvili, G. Fan, C.M. Klapperich, A.L. Furst, Surface requirements for optimal biosensing with disposable gold electrodes, ACS Meas. Sci. Au 2 (2022) 91–95, https://doi.org/10.1021/acsmeasuresciau.1c00042.
[22] S.K. Arya, P. Estrela, Recent advances in enhancement strategies for electrochemical ELISA-based immunoassays for Cancer biomarker detection, Sensors 18 (2018) 2010, https://doi.org/10.3390/s18072010.
[23] P. Fanjul-Bolado, M.B. González-García, A. Costa-García, Amperometric detection in TMB/HRP-based assays, Anal. Bioanal. Chem. 382 (2005) 297–302, https://doi.org/10.1007/s00216-005-3084-9.
[24] T. Pedersen, P. Fojan, A.K.N. Pedersen, N.E. Magnusson, L. Gurevich, Amperometric biosensor for quantitative measurement using Sandwich immunoassays, Biosensors 13 (2023) 519, https://doi.org/10.3390/bios13050519.
[25] E.-H. Yoo, S.-Y. Lee, Glucose biosensors: an overview of use in clinical practice, Sensors (Basel) 10 (2010) 4576, https://doi.org/10.3390/s100504558.

[26] S. Gao, J.M. Guisán, J. Rocha-Martin, Oriented immobilization of antibodies onto sensing platforms - a critical review, Anal. Chim. Acta 1189 (2022) 338907, https://doi.org/10.1016/j.aca.2021.338907.
[27] A. Sassolas, L.J. Blum, B.D. Leca-Bouvier, Immobilization strategies to develop enzymatic biosensors, Biotechnol. Adv. 30 (2012) 489–511, https://doi.org/10.1016/j.biotechadv.2011.09.003.
[28] N. Sandhyarani, Chapter 3 - Surface modification methods for electrochemical biosensors, in: A.A. Ensafi (Ed.), Electrochemical Biosensors, Elsevier, 2019, pp. 45–75, https://doi.org/10.1016/B978-0-12-816491-4.00003-6.
[29] R. Sánchez-Salcedo, R. Miranda-Castro, N. De-Los-Santos-Álvarez, M.J. Lobo-Castañón, D.K. Corrigan, Comparing nanobody and aptamer-based capacitive sensing for detection of interleukin-6 (IL-6) at physiologically relevant levels, Anal. Bioanal. Chem. 415 (2023) 7035–7045, https://doi.org/10.1007/s00216-023-04973-4.
[30] I. Ciani, H. Schulze, D.K. Corrigan, G. Henihan, G. Giraud, J.G. Terry, A.J. Walton, R. Pethig, P. Ghazal, J. Crain, C.J. Campbell, T.T. Bachmann, A.R. Mount, Development of immunosensors for direct detection of three wound infection biomarkers at point of care using electrochemical impedance spectroscopy, Biosens. Bioelectron. 31 (2012) 413–418, https://doi.org/10.1016/j.bios.2011.11.004.
[31] I. Horcas, R. Fernández, J.M. Gómez-Rodríguez, J. Colchero, J. Gómez-Herrero, A. M. Baro, WSXM: a software for scanning probe microscopy and a tool for nanotechnology, Rev. Sci. Instrum. 78 (2007) 013705, https://doi.org/10.1063/1.2432410.
[32] N. Elgrishi, K.J. Rountree, B.D. McCarthy, E.S. Rountree, T.T. Eisenhart, J. L. Dempsey, A practical Beginner's guide to cyclic voltammetry, J. Chem. Educ. 95 (2018) 197–206, https://doi.org/10.1021/acs.jchemed.7b00361.
[33] A. Butterworth, E. Blues, P. Williamson, M. Cardona, L. Gray, D.K. Corrigan, SAM composition and electrode roughness affect performance of a DNA biosensor for antibiotic resistance, Biosensors 9 (2019) 22, https://doi.org/10.3390/bios9010022.
[34] D. Grieshaber, R. MacKenzie, J. Vörös, E. Reimhult, Electrochemical biosensors - sensor principles and architectures, Sensors (Basel) 8 (2008) 1400–1458. https://www.ncbi.nlm.nih.gov/pmc/articles/PMC3663003/ (accessed April 27, 2023).
[35] J. Chen, K.-C. Lin, S. Prasad, D.W. Schmidtke, Label free impedance based acetylcholinesterase enzymatic biosensors for the detection of acetylcholine, Biosens. Bioelectron. 235 (2023) 115340, https://doi.org/10.1016/j.bios.2023.115340.
[36] M.P. Chatrathi, J. Wang, G.E. Collins, Sandwich electrochemical immunoassay for the detection of staphylococcal enterotoxin B based on immobilized thiolated antibodies, Biosens. Bioelectron. 22 (2007) 2932–2938, https://doi.org/10.1016/j.bios.2006.12.013.
[37] L. Steel, A.C. Ward, C. Jeffrey, D. Alcorn, D.K. Corrigan, Towards simple, rapid point of care testing for clinically important protein biomarkers of sepsis, SCIOL Biotechnology 1 (2017) 1–8. https://sciol.org/articles/biotechnology/fulltext.php?aid=sbt-1-001 (accessed December 13, 2024).
[38] A.G. Katrukha, A.V. Bereznikova, T.V. Esakova, K. Pettersson, T. Lövgren, M. E. Severina, K. Pulkki, L.M. Vuopio-Pulkki, N.B. Gusev, Troponin I is released in bloodstream of patients with acute myocardial infarction not in free form but as complex, Clin. Chem. 43 (1997) 1379–1385.
[39] A.G. Katrukha, A.V. Bereznikova, V.L. Filatov, T.V. Esakova, O.V. Kolosova, K. Pettersson, T. Lövgren, T.V. Bulargina, I.R. Trifonov, N.A. Gratsiansky, K. Pulkki, L.-M. Voipio-Pulkki, N.B. Gusev, Degradation of cardiac troponin I: implication for reliable immunodetection, Clin. Chem. 44 (1998) 2433–2440, https://doi.org/10.1093/clinchem/44.12.2433.
[40] A. Dobrea, N. Hall, S. Milne, D.K. Corrigan, M. Jimenez, A plug-and-play, easy-to-manufacture fluidic accessory to significantly enhance the sensitivity of electrochemical immunoassays, Sci. Rep. 14 (2024) 14154, https://doi.org/10.1038/s41598-024-64852-5.
[41] A. Villalonga, I. Estabiel, A.M. Pérez-Calabuig, B. Mayol, C. Parrado, R. Villalonga, Amperometric aptasensor with sandwich-type architecture for troponin I based on carboxyethylsilanetriol-modified graphene oxide coated electrodes, Biosens. Bioelectron. 183 (2021) 113203, https://doi.org/10.1016/j.bios.2021.113203.
[42] Y. Meng, Y. Li, S. Liu, S. Wang, H. Dong, F. Jiang, Q. Liu, Y. Li, Q. Wei, Sandwich-type electrochemical immunosensor based on CuFe2O4-Pd for cardiac troponin I detection, Microchim. Acta 190 (2023) 249, https://doi.org/10.1007/s00604-023-05831-x.
[43] M. Li, Y. Wu, C. Ke, Z. Song, M. Zheng, Q. Yu, H. Zhu, H. Guo, H. Sun, M. Liu, An ultrasensitive unlabeled electrochemical immunosensor for the detection of cardiac troponin I based on Pt/Au–B,S,N-rGO as the signal amplification platform, Talanta 270 (2024) 125546, https://doi.org/10.1016/j.talanta.2023.125546.
[44] X. Zhang, Q. Shang, F. Jiang, H. Dong, Y. Li, S. Wang, F. Tang, Q. Liu, Y. Li, Q. Wei, Triple signal-enhancing sandwich-type electrochemical immunosensor based on Au@SNHC and PtPdCu/BNC for detection of cardiac troponin I, Bioelectrochemistry 154 (2023) 108512, https://doi.org/10.1016/j.bioelechem.2023.108512.
[45] A.-Y. Zha, Q.-B. Zha, Z. Li, H.-M. Zhang, X.-F. Ma, W. Xie, M.-S. Zhu, Surfactant-enhanced electrochemical detection of bisphenol a based on au on ZnO/reduced graphene oxide sensor, Rare Metals 42 (2023) 1274–1282, https://doi.org/10.1007/s12598-022-02172-1.
[46] P. Yáñez-Sedeño, S. Campuzano, J.M. Pingarrón, Pushing the limits of electrochemistry toward challenging applications in clinical diagnosis, prognosis, and therapeutic action, Chem. Commun. 55 (2019) 2563–2592, https://doi.org/10.1039/C8CC08815B.
[47] H.-J. Li, Y. Huang, S. Zhang, C. Chen, X. Guo, L. Xu, Q. Liao, J. Xu, M. Zhu, X. Wang, D. Wang, B. He, S-scheme porphyrin covalent organic framework heterojunction for boosted Photoelectrochemical immunoassays in myocardial infarction diagnosis, ACS Sens. 8 (2023) 2030–2040, https://doi.org/10.1021/acssensors.3c00246.
[48] D. Beduk, T. Beduk, A.A. Lahcen, V. Mani, E.G. Celik, G. Iskenderoglu, F. Demirci, S. Turhan, O. Ozdogan, S. Ozgur, T. Goksel, K. Turhan, K.N. Salama, S. Timur, Multiplexed aptasensor for detection of acute myocardial infraction (AMI) biomarkers, Sens. Diagn. 3 (2024) 1020–1027, https://doi.org/10.1039/D4SD00010B.
[49] S.-Y. Cen, X.-Y. Ge, Y. Chen, A.-J. Wang, J.-J. Feng, Label-free electrochemical immunosensor for ultrasensitive determination of cardiac troponin I based on porous fluffy-like AuPtPd trimetallic alloyed nanodendrites, Microchem. J. 169 (2021) 106568, https://doi.org/10.1016/j.microc.2021.106568.
[50] S. Kakkar, S. Chauhan, M. Bharti, V. Bhalla Rohit, Conformational switching of aptamer biointerfacing graphene-gold nanohybrid for ultrasensitive label-free sensing of cardiac troponin I, Bioelectrochemistry 150 (2023) 108348, https://doi.org/10.1016/j.bioelechem.2022.108348.
[51] J. Ma, L. Feng, J. Li, D. Zhu, L. Wang, S. Su, Biological recognition-based electrochemical Aptasensor for point-of-care detection of cTnI, Biosensors 13 (2023) 746, https://doi.org/10.3390/bios13070746.
[52] E. Zapp, D. Brondani, T.R. Silva, E. Girotto, H. Gallardo, I.C. Vieira, Label-free Immunosensor based on liquid crystal and gold nanoparticles for cardiac troponin I detection, Biosensors 12 (2022) 1113, https://doi.org/10.3390/bios12121113.
[53] K.J. Land, D.I. Boeras, X.-S. Chen, A.R. Ramsay, R.W. Peeling, REASSURED diagnostics to inform disease control strategies, strengthen health systems and improve patient outcomes, Nat. Microbiol. 4 (2019) 46–54, https://doi.org/10.1038/s41564-018-0295-3.
[54] B.D. Mansuriya, Z. Altintas, Enzyme-free electrochemical Nano-Immunosensor based on graphene quantum dots and gold nanoparticles for cardiac biomarker determination, Nanomaterials (Basel) 11 (2021) 578, https://doi.org/10.3390/nano11030578.
[55] S. James, M. Flodin, N. Johnston, B. Lindahl, P. Venge, The antibody configurations of cardiac troponin I assays may determine their clinical performance, Clin. Chem. 52 (2006) 832–837, https://doi.org/10.1373/clinchem.2005.064857.
[56] A.V. Orlov, J.A. Malkerov, D.O. Novichikhin, S.L. Znoyko, P.I. Nikitin, Multiplex label-free kinetic characterization of antibodies for rapid sensitive cardiac troponin I detection based on functionalized magnetic Nanotags, Int. J. Mol. Sci. 23 (2022) 4474, https://doi.org/10.3390/ijms23094474.